

PV Temperature Prediction in BIPV, BAPV, BIPV/T During any Day Based on a Generalized Expression of the Ross Coefficient

S. Kaplanis^{1,*}, E.Kaplani², D.V.Bandekas³ and Despina D.Banteka⁴

¹ Renewable Energy Systems Lab, University of Peloponnese, Greece

² School of engineering, UEA, UK

³ Physics Department, International Hellenic University

⁴ University of Nicosia, Cyprus

Received 30 September 2022; Accepted 10 November 2022

Abstract

The PV temperature, T_{pv} , in a BIPV and BIPV/T structures was studied experimentally and theoretically. For this a holistic formula was used based on the Ross coefficient prediction under any environmental conditions accounting additionally for the building thermal parameters. It was shown that the slope of the PV temperature, T_{pv} , vs the solar radiation, I_T , on the BIPV modules corresponds to a generalized expression of the Ross coefficient, f , which must account for the BIPV thermal conditions, too. The profiles of the Ross coefficient for BIPV/T, BAPV and free standing PV operating in the same site were determined, compared and discussed. The theoretical and experimental analysis of a BIPV/T test cell disclosed that T_{pv} vs I_T is a linear function in all cases from sunrise till solar noon with a practically constant slope and coefficient of determination, $R^2 > 0.96$. Correspondingly, from noon to sunset the linearity still holds but with a lower slope which depends on the insulation of the building and the increased ambient temperature during sunset compared to sunrise, which is the usual case. An improved version of a T_{pv} prediction holistic formula was developed to take into account the building thermal parameters, the ratio of the PV surface over the building surface, and the environmental parameters. This new and improved methodology for the f and T_{pv} prediction for both morning to noon and noon to sunset periods was tested against measured T_{pv} vs I_T and the predicted results confirmed its validity.

Keywords: BIPV, BIPV/T, BAPV, PV temperature prediction, Ross coefficient

1. Introduction

Various papers have been published on how the ambient and PV temperatures, T_a and T_{pv} , respectively, along with the wind speed on the modules, v_w , affect the PV efficiency, η_{pv} , and performance. In addition, T_{pv} itself is considered as an implicit function in the T_{pv} prediction. The importance of the effect of the above factors as well as the module geometry and mounting configuration in the T_{pv} prediction is shown theoretically by proposed formulas [1-4], or by formulas based on ANN [5] or by simulation models [6,7]. Measured T_{pv} in various conditions and structures have been compared with predicted values obtained from simulation models [8-11]. The competitive formulae must take into account the various environmental factors and the details of the PV mounting, either BIPV integrated in the roofs or facades making an inseparable part with the building shell or adapted on the roof, BAPV, not making an inseparable part of the building or acting as sunshades or placed upon the terrace either as fixed arrays or small sun-tracking PV. An improved holistic formula [12] tested in free standing, BAPV and some BIPV configurations in various countries achieved an accurate T_{pv} prediction score within a margin $\pm(2-3)^\circ\text{C}$ around the measured T_{pv} lying between 40°C - 80°C , the latter value in fully integrated BIPV. The T_{pv} effect on the performance of BIPV and BAPV configurations was also studied by building detailed simulation models to predict the

PV output at transient and steady state conditions and for any environmental conditions [10,13-16]. The simulation model [13] predicted successfully the PV semiconductor temperature, T_c , as well as the temperatures in the front and back sides, T_f and T_b , respectively, in free standing PV, BAPV and BIPV configurations. Because T_f, T_b, T_c differ within a small range of up to 3°C they are represented by T_{pv} , which is a general notion of the PV cell/module temperature, T_c , in this text. Other simulation models successfully predicted T_{pv} in PV building configurations [17,18], in BIPV or BAPV structures such as, roofs [19,20], facades [21-25], operating under given field conditions and BIPV/T [26-28], too. However, in all the T_{pv} prediction formulas so far there was no discrimination between the 2 time periods, morning to noon and noon to sunset as far as T_{pv} in BIPVs is concerned.

In Section 2, free standing PV, BIPV operating as BIPV/T as well as BAPV designs in the form of PV Fixed and Sun Tracking (ST) adapted on the terrace are outlined. The target is to get an insight of the Ross coefficient [29], f , whose profiles are argued under various conditions. In Section 3, a theoretical analysis on the coefficient f for the fully integrated BIPV is outlined. The linearity of T_b vs I_T or T_c vs I_T in contrast to those of BAPV or free-standing PV is argued, too. Results on predicted f for BIPV/T for s.r. to noon and noon to s.s. periods are given and further discussed and interpreted in Section 4.

The Energy Balance Equation, EBE, applied to free standing PV and BAPV gives for T_{pv} [1],

*E-mail address: kaplanis@uop.gr

ISSN: 1791-2377 © 2022 School of Science, IHU. All rights reserved.

doi:10.25103/jestr.155.06

$$T_{pv} = T_a + f \cdot I_T \quad (1)$$

Eq.(1) may take a generalized form for BIPV, BIPV/T installations as argued in Section 3.

$$T_{pv} = T_{ref} + f_{BIPV} \cdot I_T \quad (2)$$

T_{ref} is a reference temperature defined in Section 3 in the study of BIPV and BIPV/T. f and f_{BIPV} correspond to eq.(3) below related to the NOCT model [29,30] and depend on the PV mounting, geometry and field conditions which in general differ from the SOC. Consequently, f at NOCT and f_{BIPV} values may differ by large, as to be shown later.

$$F_{NOCT} = (T_{NOCT} - 20^\circ C) / 800 W/m^2 \quad (3)$$

f in eqs.(1,2) is not constant. It depends on environmental, electrical and physical quantities and takes values from 0.015 to 0.045 m^2K/W in free PV or BAPV on the roof, I or terrace. The lower limit corresponds to cases where $v_w > 6m/s$, while the upper limit to cases of $v_w < 1m/s$ with the modules in low inclination, β . In BIPV roofs or facades, f lies generally in the range $[0.027 \text{ to } 0.060] m^2K/W$ with the upper limit corresponding to fully integrated PV with $v_w < 1m/s$ and low β . F depends, also, on T_{pv} through its effect on η_{pv} and U_{pv} and on β . In addition, v_w has an impact on f and T_{pv} and plays a significant role in the efficiency and power degradation [1,3-5,13,31,32]. F is determined experimentally from eqs.(1,2) by using the measured I_T , T_{pv} or T_b and T_a values or the T_{ref} notion. F may, also, be predicted from the measured I_T, v_w, T_a, T_{pv} , and β , by using the proposed holistic formula outlined in Section 4.

This research aims to get an insight into the f coefficient from s.r. to s.s. following a deep investigation and predict accurately T_{pv} with the use of a formula in BIPV and BIPV/T designs discriminating between s.r. to noon and noon to s.s. not investigated so far in the literature. For this an improvement in the holistic formula outlined in the sub-Sections 4.2&4.3 will be tested and measured T_{pv} values vs predicted ones for the periods s.r. to noon and noon to s.s. in a South facing BIPV/T will be compared.

2. BIPV and BAPV configurations and the associated Ross coefficient f and T_{pv} profiles

It is very important to have an insight on how f coefficient changes with I_T , T_a , v_w , and how it depends on the architectural and geometrical design of the PV configuration. Figures 1a-d show PV design configurations which were used in this project to predict f and T_{pv} . Figure 1a shows a BIPV/T in Patra, Greece, where the modules make an integral part of the roof. The warm air between the PV back side and the planks serving as ceiling, Figure 1b, circulates through an orifice, Figure 1c, within the room due to temperature difference between PV back side and room interior. This implies a natural air flow and heat extraction from the PV. In cases of hot months the warm air is driven out naturally through the solar chimney shown at the back in Figure 1a, while cooler air enters through the North wall to replenish the exhaust warm air. Figure 1d shows a BAPV on a terrace. Both sides of the fixed and sun-tracking, (ST), PV are subject to air free flow. It is well understood that the mode of air flow differs between BIPV, BIPV/T, BAPV and free standing PV and so does the f profile.



Fig. 1. (a-c) Details on BIPV/T with PV on the roof, (d) BAPV with modules adapted on the terrace as Fixed (right in the photo) and Sun-Tracking (left in the photo) designs.

2.1 Experimental f and T_{pv} profiles in Free Standing PV and BAPV configurations

The v_w profiles in the free standing PV and BAPV have a strong effect on T_{pv} , $(T_{pv}-T_a)$ and f shown in Figures 2a-f for a fixed and a ST BAPV adapted on a terrace. The fixed BAPV, South facing with $\beta=\phi=38^\circ$, and the ST are shown in Figure 1d. The T_{pv} itself and β have a low effect to f [12,33]. Generally, f in the ST is $<$ than the fixed one, (Figures 2a,d), because β and T_{pv} are higher in the ST compared to the fixed, and in addition both (β, T_{pv}) contribute to higher h_c or U_{pv} and hence, to a lower f . Although f is lower in the ST, T_{pv} is higher because I_T on it is much higher compared to the fixed one. All these are accounted for by the T_{pv} prediction holistic formula terms outlined in sub-Section 4.2. It must be noted, also, that the f profile vs I_T in the free standing PV and BAPV is not constant, as the slope of the line is subject to changes. In January in the fixed PV f changes by 26% while in the ST by 17% due to the effect of I_T , v_w and its direction and β . In July, the change in f during the day is about 17.5% for the fixed, while for the S.T. is much lower. These changes are clear in Figures 2a, c & 2 d, f. The slope in the curves in Figure 2f, that is the f profile, changes opposite to the one in Fig.2d mainly due to the opposite v_w profile vs hour, (Figures 2b,2e).

Conclusively, f undergoes changes in both fixed and ST BAPV arrays along the day due to the combined effect of I_T , v_w and β on T_{pv} and h_c which makes the whole process complicated. f decreases with hour as I_T increases, (Figures 2 a, c). The decrease in f is due to the high v_w profile which prevails around noon-afternoon when I_T is high. For low v_w at noon, Figure 2e, the T_{pv} vs I_T curve exhibits opposite profile, (Figures 2d, f) for both BAPV fixed and ST. Indeed, at noon in January when v_w is low the ST has higher β than the fixed. So, it receives more I_T and exhibits lower f due to

the combined effect of I_T and β for low v_w . This complex pattern of interactions is accounted for by the T_{pv} prediction formula, see sub-Section 4.2.

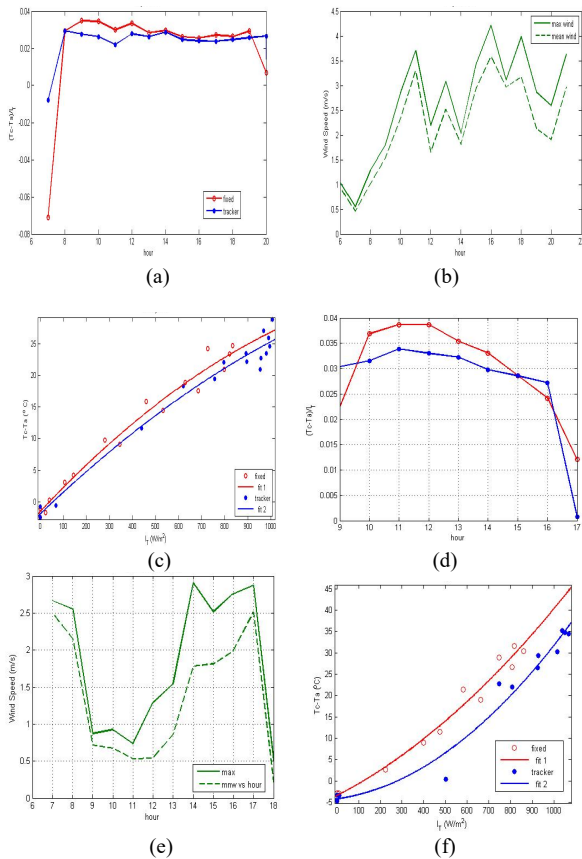


Fig. 2. (a) and (d) show f vs hour in PV fixed and ST for a day in July and January, respectively; (b) and (e) show v_w vs hour in the same day; (c) and (f) show $(T_c - T_a)$ vs I_T in the PV fixed and ST. Its slope equals the f value. The red line represents the fixed and the blue the ST.

2.2 The experimentally determined f and T_{pv} vs I_T profiles in BIPV roofs

Eq.(1) holds for free standing PV and BAPV whose both sides stand free to the air flow. On the other hand, it is important to examine the validity of eqs. (1 & 2) in BIPV designs. The measured PV back side temperature T_b is easily measured and lies very close to T_c by 1-3°C [1,13]. Therefore, both T_b , T_c are represented by the general notion T_{pv} .

The BIPV/T (Figure 1a) was monitored from Spring to Autumn and this disclosed that T_b vs I_T for the period s.r. to solar noon followed a straight line $T_b = a + bI_T$, (Fig.3a), contrary to the BAPV profiles (Figures 2a,d). The corresponding T_b vs I_T for the period noon-s.s. gives another straight line, (Figure 3b), with a lower slope than for the morning period, as discussed in Sections 3 & 4. b corresponds to f or f_{BIPV} and a to T_a or T_{ref} in eq.(2), see Section 3. a and b depend on the operating, environmental conditions and on the BIPV design, an issue argued in [20,21]. Regression analysis of the monitored data gave, as shown in Figures 3a ,b :

$a = T_{ref} = 22.12^\circ\text{C}$ and $b = f = 0.0437 \text{ m}^2\text{K/W}$ from s.r. on the PV plane to solar noon, and
 $a = T_{ref} = 35.39^\circ\text{C}$ and $b = f = 0.03685 \text{ m}^2\text{K/W}$ from noon to s.s. on the PV plane.

Those are mean values for Spring-Autumn, while the values for a specific day may differ by large according to the analysis in sub-Section 4.1, theoretically confirmed, too.

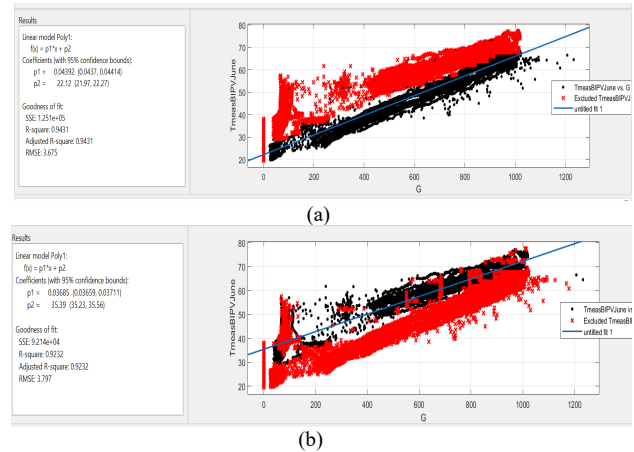


Fig. 3. Regression analysis results of T_b vs I_T data for the BIPV/T roof, Figure 1a. For s.r.-noon period, see red zone in Figure 3a; For noon-s.s. period, see black zone in Figure 3b.

2. Analysis of the T_{pv} vs I_T profiles in BIPV

2.1. The case of T_b vs I_T profiles

The analysis of the BIPV using the EBE at steady state conditions provides T_{ref} and an accurate expression of f , f_{BIPV} , determined from eq.(4a), or from the slope as in Figs.3a,b, or theoretically from eq.(4b), as outlined in sub-Section 4.2.

$$f_{BIPV,b} = (T_b - T_{ref}) / I_T, \quad \text{or} \quad (4a)$$

$$f = (1 - \eta_{pv}) / U_{pv} \quad (4b)$$

For any BAPV design and free standing PV the f values do not differ by much provided they operate under the same conditions. However, for BIPV configurations the margin of the f values may be broader because it also, depends on the building insulation, the T_a in the morning and in the sunset as well as the temperature in the building interior, T_{in} , to be proven below. In BIPV, f depends also, on I_T and $T_{pv}(I_T, v_w)$ where v_w is the wind speed on the front side and to a lower degree on β . For free standing PV and BAPV, T_b vs I_T is more sensitive to the change in the environmental conditions and the slope is not constant, (Figs.2 a, d) contrary to (Figs.3a,b). Therefore, in BIPV f depends to a lesser degree on the environmental conditions compared to the free standing and BAPV while a major role plays the building thermal properties as the analysis below and the Results show.

For a BIPV/T, T_{ref} in eq.(2) is formulated by applying the EBE on the PV module:

$$(1 - \eta_{pv}) A_{pv} I_T = U_b A_{pv} (T_b - T_{in}) + U_f A_{pv} (T_f - T_a) \quad (5)$$

T_{in} is the temperature in the building which the PV is mounted on. Let $T_b - T_f = \Delta T$, where

$$\Delta T = 1-3^\circ\text{C}, \text{ aforementioned. By substituting } \Delta T \text{ into eq.(5), } T_b \text{ is given by eq.(6)}$$

$$T_b = [T_{in} U_b + T_a U_f + U_f \Delta T] / (U_b + U_f) + ((1 - \eta_{pv}) / (U_f + U_b)) I_T \quad (6)$$

The bracket in eq.(6) corresponds to

$$T_{ref} = [T_{in} U_b + T_a U_f + U_f \Delta T] / (U_b + U_f) \quad (6a)$$

$$\text{So, } T_b = T_{ref} + f_{BIPV,b} \cdot I_T \quad (7)$$

In the morning, provided that $T_{in}=T_a$, eq.(7) becomes $T_b=T_a + f_{BIPV,b} \cdot I_T$. Hence, it approaches eq.(1). $f_{BIPV,b}$ defined in eq.(4a) equals the slope in T_b vs I_T for BIPV, (Figures 3a,b) and (Figures 4a-e), where the slope is constant from s.r. to solar noon in BIPV, while from noon to s.s. the slope is constant but lower, in general, (Figure 4f). Therefore, T_b decreases in a lower rate and does not get at sunset its value in the morning but reaches at a value $T_{ref}>T_{a,s.s}$. This is a thermal hysteresis effect due to the thermal inertia of the building itself, the module and the ground. After solar noon, T_b starts decreasing linearly till s.s. However, till 13h solar time T_b undergoes a thermal inertia due to the thermal capacity of the building and of the modules. So, it is after 800W/m² that T_b decreases with a constant rate till the sun sets on the PV plane, as it is shown by $T_{pv}-T_a=DT$ vs I_T in Fig.5. This linear behaviour was reported in [20,21] but it did not discriminate between s.r.-noon and noon - s.s periods.

3.2 The T_c vs I_T profile for BIPV

Although T_c is not easily measured compared to T_b , however, for research consistency an analysis of the T_c vs I_T profile is outlined below. The EBE for an integrated BIPV structure may also be written by using the notion T_c ,

$$(1-\eta_{pv})A_{pv}I_T = (T_c-T_a)/R_{tot} \tag{8}$$

The overall heat conductance $R_{tot}^{-1} = U_r + [U_b^{-1} + U_{bd}^{-1}(A_{pv}/A_{bd})]^{-1}$ is derived by using the electric equivalent of heat flow from the modules to the environment dropping the terms of very low resistance to heat flow from the semiconductor to the front and back side. U_{bd} is the overall heat losses coefficient of the building and A_{bd} its surface area. R_{tot}^{-1} introduced in eq.(8) gives,

$$T_c = T_a + (1-\eta)I_T / [U_r + [U_b^{-1} + U_{bd}^{-1}(A_{pv}/A_{bd})]^{-1}] \tag{9}$$

Eqs.(7&9) are equivalent and give T_b and T_c respectively, i.e. the T_{pv} for the integrated BIPV. Both result to eq.(1) for $(UA)_{bd} \gg U_b A_{pv}$. Eqs.(4&9) combined give eq.(10) where a modified coefficient $f_{BIPV,c}$ is given for BIPV,

$$f_{BIPV,c} = (1-\eta) / [U_r + [U_b^{-1} + U_{bd}^{-1}(A_{pv}/A_{bd})]^{-1}] = f \cdot [(U_r + U_b) / (U_r + [U_b^{-1} + U_{bd}^{-1}(A_{pv}/A_{bd})]^{-1})] \tag{10}$$

$f_{BIPV,c}$ is the slope of (T_c-T_a) vs I_T in a BIPV. For a not well insulated building, that is, $U_{bd} > 1W/m^2K$ and $A_{pv} \ll A_{bd}$, the $f_{BIPV,c}$ is equal to f of a similar BAPV or free standing one, eq.(1). However, for a medium insulated building, e.g. $U_{bd} = 1W/m^2K$, $f_{BIPV,c}$ is by 13% higher than the f of the BAPV, while if $U_{bd} = 0.5W/m^2K$ $f_{BIPV,c}$ is by 26% higher than the f of a similar BAPV determined from eq.(1). The deviation depends on the $U_b A_{pv} / (UA)_b$, see eq.(10). An equivalent to $f_{BIPV,c}$ value is the $f_{BIPV,b}$ estimated from eqs.(6-7), where T_{ref} is higher than T_a in eq.(9) and that equalizes the effect of the higher slope of $f_{BIPV,c}$ derived from eq.(10).

The slope of T_c vs I_T is constant because T_a increases with I_T from s.r. to noon, while $f_{BIPV,c}$ decreases with almost the same rate. Similarly, dT_b/dI_T is roughly constant from s.r. to solar noon based on the Taylor expansion of f in its vicinity, eq.(4a),

$$dT_b/dI_T = dT_{ref}/dI_T + f_{BIPV,b} + I_T df/dI_T \tag{11}$$

Eq.(11) by using the f function of eq.(7) as given by eq.(4b) may be written,

$$dT_b/dI_T = dT_{ref}/dI_T + f_{BIPV,b} + I_T [-U_{pv}^{-1} d\eta/dI_T - (1-\eta)U_{pv}^{-2} dU_{pv}/dI_T] \tag{12}$$

dT_{ref}/dI_T increases by 8-10%/100W/m² from morning to noon estimated by introducing proper data into the 1st term of eq.(6). Substituting dU_{pv}/dI_T by $(dU_{pv}/dT)(dT/dI_T)$ and $d\eta/dI_T$ by,

$$(d\eta/dT) (dT/dI_T) = -0.005 \times \eta_{pv} \times f \tag{13}$$

and setting into eq.(11) the average value of $(dU_{pv}/dT) = 0.127W/m^2K$ per K, [12], the 3rd term in eq.(11) for $\eta_{pv} = 0.15$ and $U_{pv} = 10-15W/m^2K$ equals $-f_{BIPV,b} \cdot I_T \cdot 0.05$ to $-f_{BIPV,b} \cdot I_T \cdot 0.1$ which implies that $f_{BIPV,b} \cdot I_T$ decreases by 5-10% balancing the increase in T_{ref} . After all, dT_b/dI_T for I_T within $[0, 10^3W/m^2]$ is considered practically constant between s.r. to solar noon and is subject to slight changes when v_w and/or I_T change significantly, Fig.4c. Therefore, in the morning - noon interval the slope T_b vs I_T according to eq. (11) equals $f_{BIPV,b} = \text{constant}$

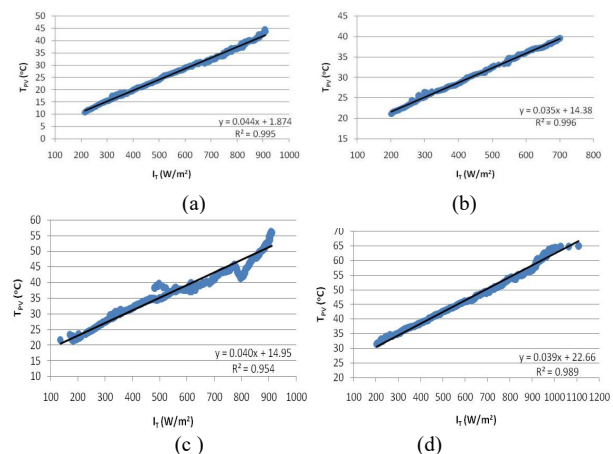
$$dT_b/dI_T = f_{BIPV,b} = \text{const} \tag{14}$$

3. Results and Discussion

3.1 T_b vs I_T profiles and Results of the f coefficient for morning and afternoon periods

One may argue that when the BIPV starts operating T_{ref} is equal to $T_a = T_{in}$. Experimentally it was confirmed that the slope of T_b or T_c vs I_T is constant from morning to noon and represents f_{BIPV} . The fluctuations of f for the morning-noon period due to the changes in T_a , v_w and I_T lie in a narrow margin, (Figures 4a-e). Similarly, the slope is constant for the afternoon period but with a lower value which implies that $f_{BIPV,b}$ in the noon- s.s period is lower than the morning one. It is very important to predict $f_{BIPV,b}$ for the noon-s.s. period, too.

The analysis in sub-Section 3.1 may interpret the lower slope of the T_b vs I_T for the period noon to s.s. (Figure 4f). This is because the T_{in} in the afternoon is higher than T_a due to the thermal heat capacity of the building and also, because the T_a profile has a lower decrease rate due to the heat capacity of the ground. Hence, $T_{a,ss} > T_{a,s.r.}$. The constant slope of T_b vs I_T is attributed in one part to the reduced v_w effect in BIPV compared to BAPV and free standing ones, and on the other, because while T_a increases from morning to noon, f decreases as T_b and I_T increase. So, they counteract each other as shown theoretically above. The fitting of T_b data on $a + bI_T$ as shown (Figures 4a-f) has a high R^2 statistic > 0.954 .



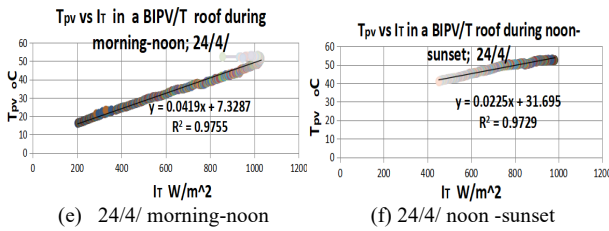


Fig. 4. T_b vs T_T of a BIPV/T roof. The $f_{BIPV,b}$ for the s.r.- noon period is written in each Figure. (a) stands for 18/3, (b) 17/5, (c) 4/10, (d) 9/7, (e) 24/4 while (f) stands for the noon-sunset in 24/4. Figure 4c shows deviations from the straight line due to strong changes in the environmental conditions. Figure 4f shows lower slope due to the afternoon period.

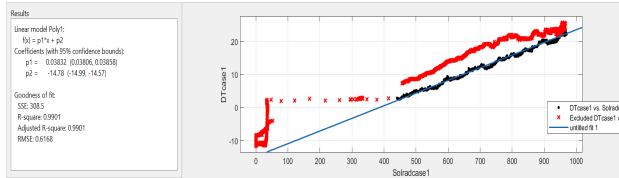


Fig. 5. $DT=T_b-T_a$ vs I_T for a BIPV during the period before and after solar noon in a cold Winter day, 28.12. $f_{BIPV,b}$ is 0.038 in the morning period and 0.037 in the afternoon till s.s.

Analysis of T_{pv} vs I_T data from a clear or almost clear sky day in every month gave an average $f=0.040$ spanning from 0.0359 till 0.045 m^2K/W , with standard deviation, $\sigma_f=0.003$. Therefore, for a 99.7% confidence level, $3\sigma_f = 0.009$, or $0.031 < f < 0.049$, i.e. the range all f values fall in.

In addition, the margin of the slopes (Figures 3a,b) is estimated between 0.052 and 0.034. That implies an estimated deviation from the mean $\delta f = \pm 0.009$ which further implies that f lies from $0.043-0.009=0.033$ to $0.043+0.009=0.052$, very close to the boundaries obtained from the 12 values one for each month, as analyzed above.

Finally, data as from Figure 4f gave an average for the noon-s.s period, $f_{12-s.s}=0.0283m^2K/W$

The difference $f_{s.r.-12} - f_{12-s.s.} = 0.040-0.028=0.012$ which is the mean annual difference.

The above imply that during the year f_{BIPV} lies within a large margin of values. In any case, T_{pv} satisfies the equation $T_{pv}=T_{ref} + f_{BIPV,b}I_T$ and $f_{BIPV,b}$ is split in 2 parts one for the morning period and the other for the afternoon.

T_{ref} is practically equal to T_a in the morning while for the afternoon period it must be estimated from eq.(6) as shown below by using the notion of T_{in} from eq.(7) for any time.

$f_{BIPV,b}$ for the s.r.-noon period in BIPV or BIPV/T, may be obtained from the f value predicted by eqs.(15-17) multiplied with the special adaptation factor SF, as detailed in sub-Section 4.2. $f_{BIPV,b}$ for the noon - s.s. period is estimated by a method based on eqs.(15-17) and on T_{ref} , T_{in} as described analytically at the points 7&8 in sub-Section 4.3.

4.2 The holistic formula to predict f and $f_{BIPV,b}$

It is important to capitalize the investigation so far concerning the prediction of T_{pv} and f for any time of a day by using a formula and a simple methodological approach suitable to BIPV configurations. The f prediction is based on a holistic formula which addresses the BIPV issues at steady state conditions. The formula is developed by factorizing f where each one factor addresses a specific environmental, geometrical and electrical parameter affecting f and T_{pv} . The complete analysis is outlined in [12], where all parameter values are provided. According to that, for natural air flow or for $v_w < 1.5m/s$,

$$f = f(v_w) \left(1 - \frac{\left(\frac{\partial \eta_{pv}}{\partial T_{pv}} \right) \delta T_{pv} + \left(\frac{\partial \eta_{pv}}{\partial I_T} \right) \delta I_T}{(1 - \eta_{pv,SOC})} \right) \left(1 - \frac{\left(\frac{\partial U_f}{\partial T_{pv}} \right) \delta T_{pv} + \left(\frac{\partial U_b}{\partial T_{pv}} \right) \delta T_{pv} + \left(\frac{\partial U_f}{\partial \beta} \right) \delta \beta + \left(\frac{\partial U_b}{\partial \beta} \right) \delta \beta}{U_{pv,SOC}} \right) \quad (15)$$

while for forced convection or for $v_w > 1.5m/s$ f is estimated by the following expression,

$$f = f(v_w) \left(1 - \frac{\left(\frac{\partial \eta_{pv}}{\partial T_{pv}} \right) \delta T_{pv} + \left(\frac{\partial \eta_{pv}}{\partial I_T} \right) \delta I_T}{1 - \eta_{pv,SOC}} \right) \quad (16)$$

$f(v_w)$ has the form of a rational function, eq.(17), which reflects the effect of v_w on T_{pv} , U_f and U_b . Its parameters correspond to the SOC values and are used as a reference to correct f due to the field deviations from SOC, that is: $\delta T_a = T_a - 20^\circ C$, $\delta I_T = I_T - 800W/m^2$, and in general $\delta \beta = \beta - 38^\circ$. Data regression analysis from an 8 years old pc-Si module gave for $f(v_w)$,

$$f(v_w) = \frac{a + bv_w}{1 + cv_w + dv_w^2} \quad (17)$$

$$a = 0.0375, b = 0.0081, c = 0.2653, d = 0.0492.$$

Eqs.(15-17) determine f for free standing PV and BAPV, where T_{pv} is calculated at steady state by the formula $T_{pv} = T_a + \Gamma_T$.

For BIPV, BIPV/T structures f from eqs.(15-17) must be multiplied with a special adaptation factor SF, in order to obtain $f_{BIPV,b} = SF \cdot f$ and then, $T_{pv} = T_b = T_{ref} + f_{BIPV,b} \cdot I_T$. More specifically:

1. $SF=1$ for BAPV or partially integrated BIPV and PV sunshades, provided that air may flow free past both module sides. So, eqs.(15-17) are also valid for such designs.
2. For BIPV and BIPV/T integrated into a roof, Figs.1a-c, f from eqs.(15,16) is multiplied with $SF=1.18$ for natural flow or when $v_w < 1.5m/s$ and $SF=1.35$ for forced flow or $v_w > 1.5m/s$ in order to provide $f_{BIPV,b}$.
3. In case the gap between the PV modules and the wall or tiles is narrow, 1-3cm, $SF=1.88$.
4. In a BIPV, BIPV/T well insulated in the front side by means of transparent vacuum or in the back side [12,21,23] the f value given by eqs.(15-17) must be multiplied by 2 to provide $f_{BIPV,b}$, since U_{pv} is practically halved due to insulation.

The SF factor takes into account the effect of the v_w in both PV sides and of the BIPV design characteristics on f . However, this correction is not adequate and needs one more correction to include the building thermal behaviour factors which in BIPV and BIPV/T designs plays a significant role in the T_{pv} prediction especially for the afternoon period. This correction comes through T_{ref} , see eqs.(6,6a) and eq.(7) compared to eq.(1), as provided in sub-Section 4.3.

4.3 A further Analysis, Experimental and Theoretical confirmation of f values for BIPV

1. According to the above deep investigation of f for BIPV, T_{pv} is predicted for both periods morning and afternoon by a more general expression

$$T_b = T_{ref} + f_{BIPV,b} \cdot I_T \quad (18)$$

T_{ref} is given by eq.(7), while the thermal analysis of the BIPV and BIPV/T gives,

$$T_{in}=(U_b A_{pv} T_b + (U A)_{bd} T_a) / (U_b A_{pv} + (U A)_{bd}) \quad (19)$$

T_a is the ambient temperature the time of the day T_{pv} is to be predicted. Eq.(18) takes into account the thermal parameters of the BIPV configuration through eq.(19) and predicts accurately f and T_{pv} for any BIPV or BIPV/T during any time of the day.

2. It was shown theoretically and experimentally that T_b vs I_T is a linear function for the period s.r.-noon, while for the period noon-s.s. the straight line has a lower slope, (Figures 3a,b , 6a,b). In cases where v_w changes significantly during the day and also I_T fluctuates due to clouds there are some deviations in the T_b vs I_T straight line (Figure 4c) and (Figure 6a). However, the s.r. - noon slope does not change significantly.

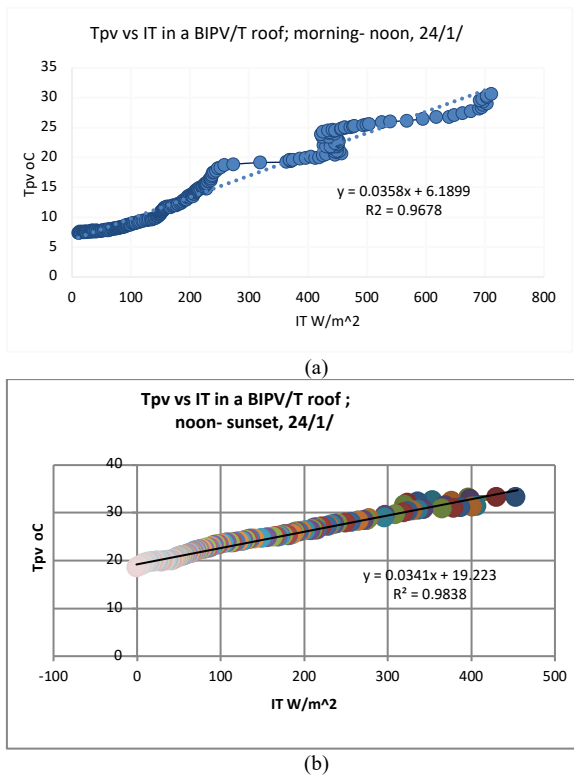


Fig. 6. (a) T_{pv} vs I_T for s.r.-noon period with severe environmental fluctuations in I_T and v_w ; (b) T_{pv} vs I_T for noon-s.s. period in the same day with normal environmental conditions.

3. The case of T_c vs I_T is not practical as T_c may not be easily measured. It was proven that,

$$T_c = T_a + f [U_r + U_b] / [U_r + [U_b^{-1} + (A_{pv}/A_{bd})/U_{bd}]^{-1}] \cdot I_T$$

T_c is very close to T_b , $T_c - T_b = \Delta T$ around 1-3°C. So, T_b may be used, instead. The expression $f [U_r + U_b] / [U_r + [U_b^{-1} + (A_{pv}/A_{bd})/U_{bd}]^{-1}]$ is the $f_{BIPV,c}$ determined from the T_c vs I_T profile.

Taking proper values of the U_{bd} and A_{pv}/A_{bd} gives that: $f_{BIPV,c} = 1.19f$ for $U_{bd} = 1$ and equal to 1.35f when $U_{bd} = 0.5$, and $A_{pv}/A_{bd} = 0.05 - 0.1$.

As U_{bd} increases, i.e. less insulated buildings, $f_{BIPV,c}$ and $f_{BIPV,b}$ approach f of a similar BAPV.

4. It is underlined that the effect of the heat losses coefficient of the building, U_{bd} , and its interior temperature, T_{in} , are accounted for in T_c vs I_T slope, and also, in the T_{ref} expression associated to T_b vs I_T in a BIPV or BIPV/T configuration.

5. f is experimentally determined from $(T_b - T_{ref})/I_T = f_{BIPV,b}$ or from $(T_c - T_a)/I_T = f_{BIPV,c}$ or it is theoretically predicted by factorizing $(1 - \eta_{pv})/U_{pv}$ as a product of factors with arguments environmental parameters and PV technical specifications, see eqs.(15-17) and multiplying with SF. The latter takes into account the effect of the different air flow mode in various BIPV, BAPV designs and structures.

6. It is underlined that T_{ref} at s.r. is equal or almost equal to $T_a = T_{in}$. So, one may use the general equation, $T_{pv} = T_a + f_{BIPV} \cdot I_T$ for the morning period. However, for the noon-sunset the slope lowers, that is, f_{BIPV} lowers because $T_{ref} > T_a$, $T_{in} > T_a$ at sunset, and also $T_{a,s,s} > T_{a,s,r}$.

7. Based on the above, the f_{BIPV} for the noon-s.s. period will be estimated and compared to the experimental one to confirm the validity of the method for the f_{BIPV} prediction at any time. So,

a. Figures 3a,b show the T_b vs I_T of the BIPV/T (Figure 1a). Data input: $T_b = 70^\circ\text{C}$ at noon and $I_T = 10^3 \text{ W/m}^2$; $A_{pv} = 0.66 \text{ m}^2$, modules specifications; $U_b = 8 \text{ W/m}^2\text{K}$, $U_f = 12 \text{ W/m}^2\text{K}$, $U_{bd} = 1 \text{ W/m}^2\text{K}$ as estimated from construction details; $A_{bd} = 20 \text{ m}^2$ technical specifications; the ambient temperatures $T_{a,s,r}$, $T_{a,12}$ and $T_{a,s,s}$ were measured 23°C , 27°C and 25°C , respectively.

For the morning-noon period $f_{BIPV,b} = (70 - 23)^\circ\text{C} / 10^3 \text{ W/m}^2 = 0.047 \text{ m}^2\text{K/W}$. The regression gave $0.044 \text{ m}^2\text{K/W}$. Data from above are substituted in eqs.(7,19) to estimate f_{BIPV} for noon-s.s.

The room interior temperature, $T_{in} = (70 \times 8 \times 0.66 + 20 \times 1 \times 25) / (8 \times 0.66 + 1 \times 20) = 34.4^\circ\text{C}$. Then, T_{ref} is determined from eq.(7): $T_{ref} = (34.4 \times 8 + 26 \times 12 + 3 \times 12) / (8 + 12) = 31.16^\circ\text{C}$. So, $f_{BIPV,b}$ for noon-s.s. = $(70 - 31.16) = 0.03824$ compared to 0.03685 from the experimental data analysis. The $f_{BIPV,b}$ and T_{ref} predicted for the noon-s.s. are very close to the results, (Figure 3b).

8. Prediction of the $f_{BIPV,b}$ in the case of the 24/1/ when the conditions of I_T and v_w strongly affected T_{pv} vs I_T . Indeed, in the s.r.-noon period (Figure 6a) the slope $f_{BIPV,b} = 0.0359$. In the noon-s.s. period the data give (Figure 6b): $T_{pv} = 32^\circ\text{C}$, T_{ref} is estimated 18°C , while $T_{a,s,s}$ was measured 15°C . The above imply that in the afternoon period $f_{BIPV,b} = (32 - 18) / 400 = 0.035$, an excellent prediction where due to hard and changing environmental conditions $f_{BIPV,b}$ for morning and afternoon did not differ much.

Based on the analysis above $T_{in} = (32 \times 8 \times 0.66 + 20 \times 15) / (8 \times 0.66 + 1 \times 20) = 18.6^\circ\text{C}$ and $T_{ref} = (18.6 \times 8 + 15 \times 12 + 3 \times 12) / (12 + 8) = 18.24$. Hence, $f_{BIPV,b}$ for the noon-s.s. period is equal to $(32 - 18.24) / 400 = 0.0344$ compared to 0.0341, (Figure 6b). These values above show the high predictive performance of the methodology to predict $f_{BIPV,b}$ for the BIPV/T throughout the day.

9. For $I_T = 800 \text{ W/m}^2$ on the BIPV/T with $\eta_{pv,STC} = 0.15$, and at present equal to 0.12 due to ageing, the uncertainty in the estimation of T_{pv} based on the experimental range $\delta f = \pm 0.001$ (Figure 3a,b) equals $\delta T_{pv} = \pm 0.001 \times 800 = \pm 0.8^\circ\text{C}$. For, $\delta \eta_{pv} / \eta_{pv} = -0.5\%$ δT_{pv} , the result is: $\delta \eta_{pv} = \pm \eta_{pv} \times 0.5\% \times 0.8^\circ\text{C} = \pm 0.12 \times 0.4\% = \pm 0.048\%$ which is really a very narrow domain for the predicted values of η_{pv} and P_m .

However, the extreme boundaries of the slope, (Figure 3a) are determined equal to 0.052 and 0.034. This implies a $\delta f = \pm 0.009$ and according to the above the extreme deviation in f derived from any season is $\delta T_{pv} = 7.2^\circ\text{C}$ which gives $\delta \eta_{pv} = \delta P_m = 0.43\%$ for any T_b vs I_T data provided by the monitoring system of the BIPV/T corresponding to any day of the year.

10. Slight deviations from the linearity due to strong changes in the environmental conditions appear (Figure 4c) and (Figure 6a) which were also observed in [31,33]. However, the linearity holds and the slope is kept within the margin argued above.

11. T_b vs I_T for a whole season in the BIPV/T is shown (Figure 7). The regression analysis gives slope equal to $0.044 \text{ m}^2\text{K/W}$ and $T_{ref} = 26^\circ\text{C}$. Figure 7 is very similar to Figure 3 in [20] which corresponds to a BAPV with modules' tilt $\beta = 15^\circ$ the same with the roof in Figure 1a. The slope of T_b vs I_T as reported in [20] is $0.02818 \text{ m}^2\text{K/W}$. The analysis below proves that both the above f values are equivalent and shows how the one is converted to the other.

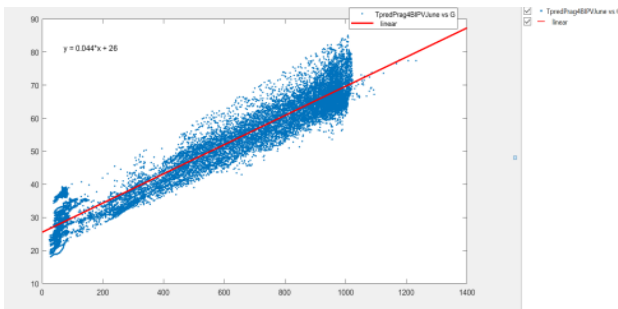


Fig 7. T_b vs I_T in the BIPV/T (Figure 1a). Data from the monitoring system in a year.

To show the equivalence of both f above for the BIPV/T and BAPV in Greece and France, respectively, one must convert the f of the latter to the BIPV/T multiplying with 1.35 as the v_w in the BIPV/T was $> 1.5 \text{ m/s}$. A correction factor due to ageing must also be introduced estimated equal to 1.0196 see [12] because the modules in the BIPV/T are 25 years old compared to the new ones in [20]. Another correction factor due to the difference in the module η_{pv} is introduced, too. $\eta_{pv} = 11.5\%$ at SOC in [20] and 9.5% for the BIPV/T in [12]. This correction factor is equal to $(1 - \delta \eta_{pv} / \eta_{pv}) = (1 - (0.095 - 0.115) / 0.115) = 1.174$. Hence, $f_{BIPV,b} = 0.02818 \times 1.35 \times 1.0196 \times 1.1739 = 0.0455$ which differs from 0.044 by 3.4%. An excellent prediction considering that it involves conversion from BAPV to BIPV in Greece and France.

12. The analysis of T_b vs I_T in sub-Chapter 3.1 formulated the notions of T_{ref} and T_{in} and through them the 2 slopes of the daily plot $T_{pv,pr}$ vs $T_{pv,meas}$ for a BIPV/T were disclosed. Indeed, the data plotted show a large dispersion in the middle of the $T_{pv,meas}$ axis at $35\text{--}55^\circ\text{C}$, (Figure 8). Such a dispersion does not appear in [13] (Figure 4) which presents the $T_{pv,pr}$ vs $T_{pv,meas}$ for a BAPV with excellent results. The plot in Figure 8 shows a split with an upper part which follows a straight line and corresponds to the morning period, and a lower part which corresponds to the afternoon data where for $T_{pv,meas}$ around $35\text{--}55^\circ\text{C}$ the predicted $T_{pv,pr}$ is lower. This implies a second T_b vs I_T straight line for the

afternoon with a lower slope, that is lower f . The T_{pv} prediction for BIPV, BIPV/T gets improved provided that for the afternoon period the prediction follows the approach illustrated in cases 7 & 8 above.

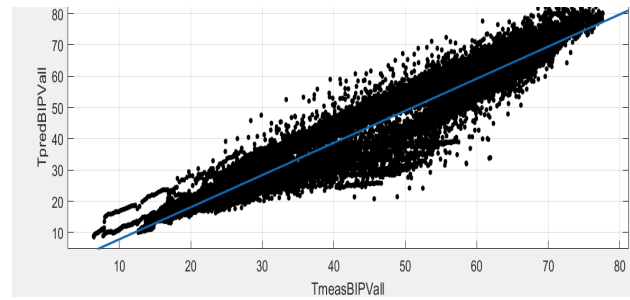


Fig. 8. T_{pv} predicted vs T_{pv} measured for the BIPV/T of Fig.1a. The slope is very near to the dichotomous 1.027 and the abscissa -2.4, with $R^2 = 0.92$.

5. Conclusions

A detailed theoretical analysis of BIPV and especially BIPV/T was outlined which showed a linear relationship between PV temperature, T_{pv} , and solar irradiation on it, I_T . For this generalized expressions were introduced where the so called Ross coefficient, f , is replaced by $f_{BIPV,b}$ and the ambient temperature, T_a , by a reference temperature, T_{ref} . The latter takes into account the heat losses coefficients of both sides of the PV modules, U_f and U_b , the thermal conductance of the building, $(UA)_{bd}$, which the PV modules are mounted on, and the temperature inside the building. Those generalized expressions were derived and used in the T_{pv} prediction formulas and in the theoretical confirmation of the experimental results, T_b vs I_T . Specifically, T_b follows a linear function with I_T from sunrise to solar noon, which is affected by any changes of the environmental conditions, but to a lower degree compared to BAPV and free standing PV. The $f_{BIPV,b}$ depends on the thermal losses of the BIPV and BIPV/T and the total area of the PV modules over the building surface. The contribution of the building thermal inertia reduces the $f_{BIPV,b}$ value during the afternoon period. A methodology was developed on how to derive the $f_{BIPV,b}$ value for the afternoon period from the $f_{BIPV,b}$ value of the morning period and confirmed the experimentally determined one. The methodology developed in this paper improves significantly the previous f and T_{pv} prediction formulas published by the authors as it adds a component on how to estimate $f_{BIPV,b}$ and T_b for the afternoon in a BIPV and BIPV/T. Successful prediction of the $f_{BIPV,b}$ and T_{pv} for the afternoon in a BIPV/T unit was shown in comparison with the experimentally determined ones. By using the methodology outlined in this article, the f coefficient in a BAPV in France was successfully converted to predict the $f_{BIPV,b}$ of a BIPV/T in Greece. The methodology outlined predicts with a very high accuracy the PV temperature for any BIPV or BIPV/T and BAPV configuration for any hour from morning to sunset for any day.

This is an Open Access article distributed under the terms of the Creative Commons Attribution License.



References

- 1.D.L. King, W.E. Boyson, J.A. Kratochvill. Photovoltaic Array Performance Model. SAND2004-3535, December 2004.
2. E. Skoplaki, A.G. Boudouvis, J.A. Palyvos J.A. A simple correlation of the operating temperature of photovoltaic modules of arbitrary mounting. *Solar Energy Materials & Solar Cells*, vol.92(2008)1393-1402
3. M. Mattei et al. (2006). Calculation of the polycrystalline PV module temperature using a simple method of energy balance. *Renewable Energy*, vol. 31(2006) 553–567.
- 4.D. Faïman (2008). Assessing the outdoor operating temperature of photovoltaic modules. *Progress in Photovoltaics: Research and Applications*, vol. 16 (2008)307–315.
5. T.G.Mani et al. Photovoltaic module thermal/wind performance: Long term monitoring and model development for energy rating. NREL/CD-520-33586,(2003)936-939
- 6.G.M.Tina, G. Marletta, S. Sardella. Multy-layer thermal models of PV modules for monitoring applications” Proceedings 38th IEEE Photovoltaic Specialists Conference,(2012), Austin, Texas, DOI:10.1109/PHOTOV.2012.6318203.
7. C.Li,S. Spataru, K.M. Zhang, Y.Yang, H.Wei. A Multi-State Dynamic Thermal Model for Accurate Photovoltaic Cell Temperature Estimation. *IEEE Journal of Photovoltaics*,(2020), DOI:10.1109/JPHOTOV.2020.2987401
8. M.U.Siddiqui, A.F. Arif , L. Kelley, and S. Dubowsky. Three-dimensional thermal modeling of a photovoltaic module under varying conditions, *Solar energy*, vol. 86,(2012), 2620-2631
- 9.S.Armstrong,W.G. Hurley. A thermal model for photovoltaic panels under varying atmospheric conditions. *Applied Thermal Engineering*, vol.30(2011)1488-1495.
10. S.Kaplanis, E. Kaplani. A New Dynamic Model to Predict Transient and Steady State PV Temperatures Taking into Account the Environmental Conditions. *Energies* vol.12 (2019)2
- 11.A.K. Abdulrazzaq, B. Plesz, G. Bogнар. A Novel Method for Thermal Modelling of Photovoltaic Modules/Cells under Varying Environmental Conditions. *Energies*, vol.13(2020) 3318
12. S.Kaplanis, E.Kaplani, J.K. Kaldellis “PV temperature and performance prediction in free-standing, BIPV and BAPV incorporating the effect of temperature and inclination on the heat transfer coefficients and the impact of wind, efficiency and ageing”.*Renewable Energy* vol.181 (2022) 235-249
- 13.E. Kaplani, S. Kaplanis, Dynamic Electro-Thermal PV Temperature and Power Output Prediction Model for Any PV Geometries in Free-Standing and BIPV Systems Operating under Any Environmental Conditions, *Energies*,vol. 13 (2020) 4743
- 14.G. Ciulla, V. Lo Brano, and E. Moreci. Forecasting the cell temperature of PV modules with an adaptive system”. *International Journal of Photoenergy*, vol. 2013, Article ID 192854; <https://doi.org/10.1155/2013/192854>
15. P.A. Shahzada et al. Using energy balance method to study the thermal behavior of PV panels under time varying field conditions. *Energy Conversion and Management*, vol.175(2018)246-262
- 16.G. Graditi, S. Ferlito, G. Adinolfi,GM Tina, C.Ventura. Energy yield estimation of thin-film photovoltaic plants by using physical approach and artificial neural networks. *Solar Energy* vol. 130(2016)232-243
17. DT Lobera, S. Valkealahti. Dynamic thermal model of solar PV systems under varying climatic conditions. *Solar Energy*, vol. 93(2013)183-194
18. Y.B. Assoa et al. Thermal Analysis of a BIPV system by various modelling approaches. *Solar Energy* 155(2017)1289-99
19. C.Toledo et al.Thermal performance of PV modules as building elements: Analysis under real operating conditions of different technologies”*Energy and Buildings*.vol.223(2020) 110087
20. M. D’Orazio, C. Di Perna, E. Di Giuseppe. Experimental operating cell temperature assessment of BIPV with different installation configurations on roofs under the Mediterranean climate. *Renewable Energy*, vol.68(2014)378-386
21. K. Vats, G.N. Tiwari . Performance evaluation of a building integrated semitransparent photovoltaic thermal system for roof and facade” *Energy and Buildings* 45(2012)211-218; <https://doi.org/10.1016/j.enbuild.2011.11.008>
22. Yen-Chieh Huang, Chi-Chang Chan, Szu-Chi Kuan, Shui-Jinn Wang, and Shin-Ku Lee “Analysis and Monitoring Results of a Building Integrated Photovoltaic Façade Using PV Ceramic Tiles in Taiwan” *Intern. J.of Photoenergy*, Vol. 2014, Article ID 615860, 12 pages <http://dx.doi.org/10.1155/2014/615860>
23. A.Ghosh, N. Sarmah, S. Sundaram, TK. Mallick. Numerical studies of thermal comfort for semi-transparent building integrated photovoltaic (BIPV)-vacuum glazing system. *Solar Energy*, vol.190(2019) 608-616.
- 24.J. Han, L. Lu, J. Peng, H. Yang. Performance of ventilated double-sided PV façade compared with conventional clear glass façade. *Energy and Buildings*, vol.56(2013) 204-209.
25. M. Shahrestan, R.Yao, E. Essah, L. Shao, AC Oliveira, A. Hepbasli, JL Lechón. Experimental and numerical studies to assess the energy performance of naturally ventilated PV façade systems. *Solar Energy*, vol.147(2017) 37-51
26. Y. B. Assoa, L. Gaillard, C. Ménézo, N. Negri, F. Sauzedde. Dynamic prediction of a building integrated photovoltaic system thermal behaviour, *Applied Energy* vol.214 (2018) 73–82, <https://doi.org/10.1016/j.apenergy.2018.01.078>
27. T.Yang, A. K. Athienitis “Performance Evaluation of Air-Based Building Integrated Photovoltaic/Thermal (BIPV/T) System with Multiple Inlets in a Cold Climate” *Procedia Engineering*. Vol.121(2015)2060-2067
28. P. Karava, CM Jubayer, E. Savory, S. Li. Effect of incident flow conditions on convective heat transfer from the inclined windward roof of a low-rise building with application to photovoltaic-thermal systems. *Journal of Wind Engineering and Industrial Aerodynamics*, vol.104(2012)428-438.
29. RG Ross. Interface design considerations for terrestrial solar cell modules. *Proceedings of the 12th IEEE Photovoltaic Specialist’s Conference*, Baton Rouge L.A.(1976)801-806,
30. International Standard IEC 61215 “Crystalline silicon terrestrial photovoltaic (PV) modules – design qualification and type approval” IEC edition, 4 April 2017
31. C. Schwingshackl et al. Wind effect on PV module temperature: Analysis of different techniques for an accurate estimation. *Energy Procedia* vol.40(2013)77-86.
32. B.J.Brinkworth, R.H.Marshall, Z. Ibarahim. A validated model of naturally ventilated PV cladding. *Solar Energy* vol.69(2000)67-81
33. E.Kaplani, S. Kaplanis. Thermal modelling and experimental assessment of the dependence of PV module temperature on wind velocity and direction, module orientation and inclination. *Solar Energy* vol.107(2014)443-460

Nomenclature

A_{pv}, A_{bd}	The area of a module and building, respectively, (m ²)	T_{SOC}, T_{NOCT}	The PV temperature when operating under SOC, NOCT (°C)
BIPV, BIPV/T	Building Integrated PV, Building Integrated PV & Thermal, respectively	U_{bd}	The overall heat losses coefficient of the building with the BIPV on it (W/m ² K)
BAPV	Building Adapted PV	U_f	heat losses coefficients due to convection and IR radiation at the front side of the PV module (W/m ² K), equal to $h_{c,f} + h_{r,f}$
I_T	Global solar radiation intensity on the PV plane (W/m ²)	U_b	heat losses coefficients due to convection and IR radiation at the back side of the PV module (W/m ² K), equal to $h_{c,b} + h_{r,b}$
NOCT	Normal Operating Cell Temperature of a PV	U_{pv}, U_{soc}	The overall heat losses coefficient= $U_f + U_{b, on a}$

	module operating under SOC		PV at SOC, inland and sea environment, respectively (W/m^2K)
P_m	Peak power of a PV module (W)	f_i	The Ross coeff. at inland site and sea environment, respectively (m^2K/W)
SF	Special adaptation factor (number)	f_{BIPV}	The f value associated to a BIPV
SOC	Standard Operating Conditions: under open circuit with $I_T=800W/m^2$, $T_a=20^\circ C$, $v_w=1m/s$ parallel to the module plan	h_c ,	Heat convection coefficient (W/m^2K)
STC	Standard Test Conditions: radiation of 1 kW/m^2 , cell temperature $25^\circ C$, $v_w=0m/s$.	s.r. s.s.	Sunrise, sunset
T_a, T_{in}	ambient temperature and interior/room temperature, respectively ($^\circ C$)	v_w	wind velocity (m/s)
$T_{a,s.r.}, T_{a,s.s.}$	T_a at sunrise and sunset on the PV plane, respectively	ΔT	T_{pv} or $T_b - T_a$
T_b, T_c, T_f	PV back side, cell semiconductor, and front side temperatures, respectively, ($^\circ C$)	β	PV module inclination angle with reference to the horizontal
T_{pv}	PV module temperature, as a general notion representing T_b, T_c, T_f by 1-3 $^\circ C$ close to each other	$\eta_{pv}, \eta_{pv,soc}$	Efficiency of the PV cell/module in general and at SOC, respectively
T_{ref}	Reference temperature, function of T_a, T_{in}, U_{pv} etc ($^\circ C$)		